

---

# Deep Ensembles for Epistemic Uncertainty: A Frequentist Perspective

---

Anchit Jain<sup>1</sup> Stephen Bates<sup>1</sup>

## Abstract

Decomposing prediction uncertainty into aleatoric (irreducible) and epistemic (reducible) components is critical for the reliable deployment of machine learning systems. While the mutual information between the response variable and model parameters is a principled measure for epistemic uncertainty, it requires access to the parameter posterior, which is computationally challenging to approximate. Consequently, practitioners often rely on probabilistic predictions from deep ensembles to quantify uncertainty, which have demonstrated strong empirical performance. However, a theoretical understanding of their success from a frequentist perspective remains limited. We address this gap by first considering a bootstrap-based estimator for epistemic uncertainty, which we prove is asymptotically correct. Next, we connect deep ensembles to the bootstrap estimator by decomposing it into data variability and training stochasticity; specifically, we show that deep ensembles capture the training stochasticity component. Through empirical studies, we show that this stochasticity component constitutes the majority of epistemic uncertainty, thereby explaining the effectiveness of deep ensembles.

## 1. Introduction

While machine learning systems are increasingly accurate in tightly-controlled settings, a key challenge to their deployment in more complex, real-world environments is uncertainty awareness—algorithms should be able to accurately report on their level of confidence or reliability in different conditions. Moreover, there are different underlying reasons for uncertainty. Uncertainty may be due to inherent unpredictability in a population with the current feature set (aleatoric or irreducible uncertainty) or instead due to limited training data (epistemic or reducible uncertainty). Distinguishing these types of uncertainty is important in

order to take the correct downstream action. High aleatoric uncertainty indicates that the current prediction task is inherently challenging, and we cannot have high confidence in any one prediction unless we are able to collect richer data (not just more data). On the other hand, high epistemic uncertainty signals that collecting more training data in this region is likely to improve the model, which makes it suitable for guiding model development and active learning (Houlsby et al., 2011; Gal et al., 2017; Smith et al., 2023). We focus on this quantity in this work.

A popular measure of epistemic uncertainty is the mutual information (MI) between model parameters and predictions which quantifies the expected reduction in uncertainty from observing new data (Houlsby et al., 2011; Depeweg et al., 2018). MI is a fundamentally Bayesian quantity that requires access to the posterior distribution over model parameters, which generally renders its exact calculation intractable. As such, substantial effort has gone into developing approximate Bayesian computational techniques (MacKay, 1995; Graves, 2011; Welling & Teh, 2011; Hernandez-Lobato & Adams, 2015; Gal & Ghahramani, 2016), but they are often difficult to scale, compromise predictive accuracy or have weak Bayesian justification.

In light of these challenges, practitioners often use deep ensembles (Lakshminarayanan et al., 2017) to obtain uncertainty estimates. Deep ensembles proceed by generating an ensemble of models by only varying the randomization in the training procedure (e.g. initial weights, data shuffling etc.). Previous works have noted that probabilistic predictions from the deep ensemble reliably quantify uncertainty and exhibit strong performance on downstream tasks (Lakshminarayanan et al., 2017; Ovadia et al., 2019; Ashukha et al., 2020). While Bayesian interpretations have been proposed (Wilson & Izmailov, 2020), a theoretical frequentist understanding behind the success of deep ensembles is lacking. Furthermore, various sources such as limited data, misspecified models or noisy optimization contribute to the uncertainty (Hüllermeier & Waegeman, 2021) and estimates may only account for some of these. Therefore, to correctly use an uncertainty estimate, it is crucial to understand the sources it captures. Our work aims to provide a frequentist perspective on the nature of epistemic uncertainty captured by deep ensembles.

<sup>1</sup>EECS, MIT, Cambridge MA, USA. Correspondence to: Anchit Jain <ajain625@mit.edu>.

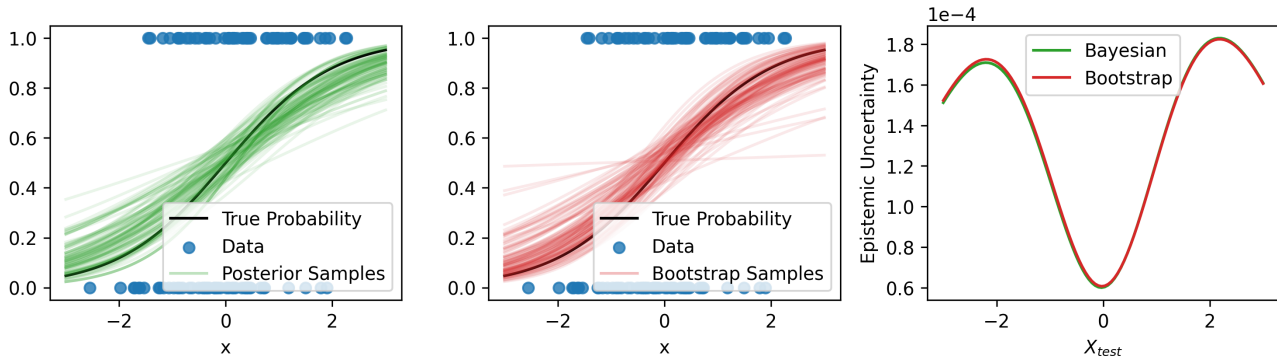


Figure 1. **Teaser Simulation:** (left) Training data, true label probability and posterior sample predictions. (center) Predictions from MLEs over bootstrapped datasets. (right) Epistemic uncertainty calculated through Bayesian inference (MCMC) versus the bootstrap estimate.

Our analysis proceeds in three parts. Firstly, we provide an asymptotic expansion for MI which links it to the Fisher information and shows how epistemic uncertainty differs from frequentist variance. We use this to motivate the construction of a bootstrap estimator which targets the MI. Secondly, since the epistemic uncertainty within a deep ensemble arises only due to the randomness in the training procedure, we decompose the bootstrap estimator into components arising due to data sampling and training randomness to facilitate comparison. Finally, through empirical studies, we note that deep ensembles capture the portion of epistemic uncertainty due to stochastic optimization, which in turn appears to be the majority component, explaining their success.

### 1.1. Our Contribution

Our contributions can be summarized as follows.

- **Link between mutual information and frequentist Fisher information:** We provide an asymptotic expansion for MI and show how it depends not only on the variance in model predictions as measured by the Fisher information, but also on the degree of randomness in the true data generating process.
- **Contributions to MI from data variability and training randomness:** We use the asymptotic expansion to construct a bootstrap estimator of MI. To allow comparison with deep ensembles, we show how this bootstrap estimator separates into components arising from training stochasticity and variability in data sampling.
- **Empirical comparison with deep ensembles:** We conduct empirical studies across a variety of deep learning tasks that show that training stochasticity is dominant over variability in data sampling, with deep ensembles capturing the latter.

### 1.2. Illustration

To provide the key intuition motivating the bootstrap estimator, we provide the following simulation. Consider a binary logistic regression model,  $\mathbb{P}(y = 1|x, \theta) = 1/(1 + e^{-\theta_1 x - \theta_0})$ . We sample the features  $x$  from a standard normal and also impose standard normal priors on  $\theta_0, \theta_1$ . Fig. 1(left) visualizes the data and the true model along with 100 posterior samples from the true Bayesian posterior, obtained using a Markov chain Monte Carlo (MCMC) algorithm. Next, we calculate maximum likelihood estimates (MLEs) for the parameters across 100 bootstrapped datasets and show these in Fig. 1(middle)—note the remarkable similarity in the posterior and bootstrap samples. Finally, we use these MCMC and bootstrap samples to form our estimate of the epistemic uncertainty as per Algorithm 1 noting the excellent agreement in Fig. 1(right). We leverage this connection to study Bayesian MI using bootstrapping, which then allows a comparison with deep ensembles.

## 2. Background

### 2.1. Mutual Information as Epistemic Uncertainty

A popular uncertainty decomposition (MacKay, 1992; Houlby et al., 2011; Depeweg et al., 2018) leverages information-theoretic quantities to propose measures of aleatoric and epistemic uncertainty. Let the random variables  $Y$  and  $X$  denote the labels and features respectively in a supervised learning setup. Let  $\mathcal{D}_n$  be the data comprising of  $n$  realizations of  $(Y, X)$ . Further, let  $\theta$  be the random variable denoting the parameters of a prediction model. Information theory states that  $H(Y)$  is the uncertainty in  $Y$  and defines mutual information as

$$\underbrace{I(Y; \theta|X, \mathcal{D}_n)}_{\text{Epistemic}} = \underbrace{H(Y|X, \mathcal{D}_n)}_{\text{Total}} - \underbrace{H(Y|\theta, X, \mathcal{D}_n)}_{\text{Aleatoric}}. \quad (1)$$

The quantification of epistemic uncertainty as the mutual information (MI) between the (test) data and parameters

is conceptually pleasing since Eq. 1 reveals it to be the reduction in label uncertainty from knowing the model parameters. This MI is a fundamentally Bayesian object since it requires  $\theta$  to be random.

## 2.2. Bootstrap

The original bootstrap procedure (Efron, 1979) was proposed to estimate the variance of an estimator under different draws of the data. Consider a setting where there are no repeated data points. Bootstrap first samples weights from a symmetric multinomial distribution with all event probabilities  $1/n$ . These weights are used to reweight the original data to create a “bootstrapped dataset” over which the estimator is recomputed. This procedure is replicated  $B$  times to obtain  $B$  “bootstrapped estimates”. The key intuition behind the bootstrap—the “plug-in” principle—proposes that the distribution of these bootstrapped estimates approximates the distribution of the original estimator under re-draws of the data. As such, we can obtain an estimate of the variance of our estimator as the empirical variance of the bootstrapped estimates.

We can also instead draw weights from a symmetric Dirichlet distribution (Rubin, 1981). We hypothesize that in a deep learning setting, these weights are more suitable since it allows the neural network to still see all the training instances and hence capture the training data better than multinomial weights which omit training points entirely. For our paper, we thus use Dirichlet weights for our experiments but emphasize that our theorems hold for multinomial weights too (Appendix A).

## 2.3. Deep Ensembles

Deep ensembles (Lakshminarayanan et al., 2017) are a simple but powerful uncertainty quantification technique for deep neural networks (DNNs). A deep ensemble is obtained by training multiple models with the exact same architecture and training data but with different random seeds controlling stochasticity in the training procedure (different parameter initializations, different data shuffling when using stochastic gradient descent etc.). The deep ensemble model prediction is simply the average of predictions of member models. They have shown success at a variety of uncertainty quantification tasks (Lakshminarayanan et al., 2017; Ovadia et al., 2019; Ashukha et al., 2020).

## 3. Algorithm and Theoretical Results

### 3.1. Problem Setup

We now specialize the previous notation to our exact setting. Consider a  $K$ -class supervised classification problem with labels  $Y \in \{1, \dots, K\}$ . Denote the training data by  $\mathcal{D}_n = \{(X_i, Y_i), i = 1, \dots, n\}$ . We wish to evaluate the epistemic

uncertainty in the prediction for the label  $Y_{\text{test}}$  given the feature  $X_{\text{test}}$ . We denote our probability predictions for  $Y_{\text{test}}$  for a model parametrized by  $\theta \in \Theta$  by  $\hat{p}(X_{\text{test}}; \theta)$ . Further, denote by  $\hat{p}_k(X_{\text{test}}; \theta)$  the prediction probability assigned to the  $k^{\text{th}}$  class. The model is specified such that  $0 < \hat{p}_k(X_{\text{test}}; \theta) < 1$  and  $\sum_{k=1}^K \hat{p}_k(X_{\text{test}}; \theta) = 1$ . Finally, we also assume that the model is well-specified, i.e., there exists a  $\theta_0 \in \Theta$  such that  $(X_i, Y_i) \stackrel{iid}{\sim} P_X(x)\hat{p}_y(x; \theta_0) =: P_{\theta_0}$

In the Bayesian setup, we have a prior  $p(\theta)$  over the parameters and we denote by  $p(\theta|\mathcal{D}_n)$  our posterior. We use the notation  $\mathbb{E}_Z[\cdot]$  to denote expectations taken with respect to the random variable  $Z$ . As per Sec. 2.1, the epistemic uncertainty is

$$\begin{aligned} & \text{I}(Y_{\text{test}}; \theta | X_{\text{test}}, \mathcal{D}_n) \\ &= \text{H}(Y_{\text{test}} | X_{\text{test}}, \mathcal{D}_n) - \text{H}(Y_{\text{test}} | \theta, X_{\text{test}}, \mathcal{D}_n) \\ &= \text{H}(\mathbb{E}_{\theta|\mathcal{D}_n}[\hat{p}(X_{\text{test}}; \theta)]) - \mathbb{E}_{\theta|\mathcal{D}_n}[\text{H}(\hat{p}(X_{\text{test}}; \theta))] \end{aligned}$$

### 3.2. Asymptotics of Mutual Information

We begin by deriving the asymptotic behavior of mutual information, connecting it with the Fisher information and frequentist sampling variation. This connection will allow us to repurpose frequentist methods for estimating variation to instead target the mutual information.

**Theorem 3.1.** *Under the assumptions needed for Bernstein von-Mises to hold and uniform integrability of the predicted probabilities (1-7 in Appendix A) we have the asymptotic expansion*

$$\text{I}(Y_{\text{test}}; \theta | X_{\text{test}}, \mathcal{D}_n) = \frac{1}{2n} \sum_{k=1}^K \frac{\sigma_k^2}{\hat{p}_k(X_{\text{test}}; \theta_0)} + o_p(n^{-1}) \quad (2)$$

$\forall X_{\text{test}}$ , where  $\sigma_k^2$  is

$$\sigma_k^2 = \left[ \frac{\partial \hat{p}(X_{\text{test}}; \theta_0)}{\partial \theta} \mathcal{I}^{-1}(\theta_0) \frac{\partial \hat{p}(X_{\text{test}}; \theta_0)}{\partial \theta} \right]_{k,k}$$

for  $\mathcal{I}^{-1}(\theta_0)$  being the inverse Fisher information of the model at  $\theta_0$ .

**Proof Sketch:** Our analysis proceeds by Taylor expanding the entropy function about the mean posterior predicted probability. We then apply the functional delta method to the Bernstein von-Mises theorem to obtain the limiting law of our predictions. Recall that the Bernstein von-Mises theorem holds under correct model specification, sufficient smoothness, identifiability, and feasibility of  $\theta_0$  under the prior (Theorem 10.1 of van der Vaart (2000)). Finally, we use uniform integrability to obtain the limiting posterior moments. We defer the full proof to Appendix A.

We briefly digress to comment on the theorem and provide better intuition for epistemic uncertainty as measured by mutual information. Firstly, the theorem shows that mutual information decreases linearly in the number of samples. Next, it connects mutual information to the Fisher information and perhaps surprisingly shows how the first order asymptotics are governed by the inverse Fisher information divided by the true conditional probabilities.

Better intuition can be gained into the first order asymptotic term by considering the binary classification case in which the first order term simplifies to

$$\frac{(\partial \hat{p}_1(X_{\text{test}}; \theta_0) / \partial \theta)^T (n^{-1} \mathcal{I}^{-1}(\theta_0)) (\partial \hat{p}_1(X_{\text{test}}; \theta_0) / \partial \theta)}{2 \hat{p}_1(X_{\text{test}}; \theta_0) (1 - \hat{p}_1(X_{\text{test}}; \theta_0))}$$

as noted in MacKay (1992). Recall that  $n^{-1} \mathcal{I}^{-1}(\theta_0)$  is the (asymptotic) variance of the MLE. The numerator in the expression above can then be interpreted as the variance of the model prediction at  $X_{\text{test}}$ .  $1/2p(1-p)$  achieves a minimum at  $1/2$  and tends to infinity at 0 and 1. The first order term is then directly proportional to the model variance but also inversely proportional to the the ground truth certainty (i.e. how close  $\hat{p}_1(X_{\text{test}}; \theta_0)$  is to 0 or 1). Thus, we see that this first order term matches the intuition behind epistemic uncertainty; if our predictions are uncertain but the true outcome is certain then we can expect to reduce our uncertainty and hence have high epistemic uncertainty.

### 3.3. A Bootstrap Estimator

Theorem 3.1 suggests that asymptotically correct estimation of the Fisher information and true model probabilities can thus be used to construct first order accurate estimators of mutual information. In light of this, we consider a bootstrap based estimator which we denote by  $I_b(X_{\text{test}}, \mathcal{D}_n)$ .

Estimation proceeds by first sampling weights  $\xi$  from the symmetric Dirichlet with concentration parameter 1. Denote the MLE of  $\theta$  over the bootstrapped dataset as  $\hat{\theta}_b$  (for example, as obtained by minimizing cross-entropy loss). We denote the distribution of this estimate (induced by the randomness in the weights) given the data  $\mathcal{D}_n$  as  $p(\hat{\theta}_b | \mathcal{D}_n)$ . Then,

$$I_b(X_{\text{test}}, \mathcal{D}_n) := \mathbb{H}(\mathbb{E}_{\hat{\theta}_b | \mathcal{D}_n} [\hat{p}(X_{\text{test}}; \hat{\theta}_b)]) - \mathbb{E}_{\hat{\theta}_b | \mathcal{D}_n} [\mathbb{H}(\hat{p}(X_{\text{test}}; \hat{\theta}_b))].$$

Algorithm 1 makes this procedure explicit for clarity.

**Theorem 3.2.** *Under the assumptions needed for Bernstein von-Mises to hold, for asymptotic normality of the MLE to hold and uniform integrability of the predicted probabilities (1-12 in Appendix A), we have*

$$\frac{I(Y_{\text{test}}; \theta | X_{\text{test}}, \mathcal{D}_n)}{I_b(X_{\text{test}}, \mathcal{D}_n)} \xrightarrow{P_{\theta_0}^n} 1 \quad \forall X_{\text{test}}.$$

---

#### Algorithm 1 $I_b(X_{\text{test}}, \mathcal{D}_n)$ estimation

---

**Input:** Number of bootstrap replications  $B$ , training dataset  $\mathcal{D}_n$

$\Theta_b \leftarrow \{\}$

**for**  $b \leftarrow 1$  **to**  $B$  **do**

**sample**  $\xi \sim \text{Dir}(1, \dots, 1)$

$\hat{\theta}_b \leftarrow \text{argmax}_{\theta \in \Theta} \sum_{i=1}^n \xi_i \log(\hat{p}_{Y_i}(X_i; \theta))$

$\Theta_b \leftarrow \Theta_b \cup \{\hat{\theta}_b\}$

**end for**

$$I_b(X_{\text{test}}, \mathcal{D}_n) = \mathbb{H}\left(\frac{1}{B} \sum_{\hat{\theta}_b \in \Theta_b} \hat{p}(X_{\text{test}}; \hat{\theta}_b)\right) - \frac{1}{B} \sum_{\hat{\theta}_b \in \Theta_b} \mathbb{H}\left(\hat{p}(X_{\text{test}}; \hat{\theta}_b)\right)$$

**Output:**  $I_b(X_{\text{test}}, \mathcal{D}_n)$

---

**Proof Sketch:** We proceed as in Theorem 3.1 but invoke bootstrap limit laws (Theorem 10.16 of Kosorok (2007)) instead of Bernstein von-Mises to obtain an identical asymptotic expansion for our estimator. We provide the complete proof in Appendix A.

We note that our theorem also holds if we use the classic multinomial weights for bootstrap instead of Dirichlet ones—see Appendix A.

Theorem 3.2 proves the asymptotic validity of the bootstrap estimator and provides a frequentist path to studying the Bayesian MI.

### 3.4. Distinguishing Algorithmic Randomness from Statistical Uncertainty

Deep neural networks are generally trained with variants of stochastic gradient descent and a random parameter initialization. As such, the fitted model is random even with the training data fixed. Deep ensembles exploit this phenomenon, effectively capturing only the epistemic uncertainty arising from training stochasticity. The bootstrap estimator in Sec. 3.3 provides the crucial conceptual link between the ad-hoc operational technique of deep ensembles and principled Bayesian inference. While standard Bayesian formulations cannot account for stochasticity in model training, in this section we show how the bootstrap estimator naturally decomposes into distinct terms for data variability and training stochasticity, providing a mechanism to isolate the latter. This decomposition will then allow us to study deep ensembles by directly comparing them to the training stochasticity component of a theoretically grounded estimator.

In more detail, the parameter estimate can be viewed as a function of the data and the random seed. Thus, for the remainder of this section, we use the notation  $\hat{p}(X_{\text{test}}; \hat{\theta}_b) = \hat{p}(\mathcal{D}_n^b, s)$  where  $\mathcal{D}_n^b$  denotes the bootstrapped dataset and  $s$  denotes the seed used for training the DNN. Since  $\hat{\theta}_b$  is deter-

ministic given  $(\mathcal{D}_n^b, s)$ ,  $\hat{p}(\mathcal{D}_n^b, s)$  is a deterministic function. Normally, the selection of  $s$  is completely independent of everything else and hence  $(s|\mathcal{D}_n^b, \mathcal{D}_n) \stackrel{d}{=} s$ .

With this notation in place, we propose the following decomposition of the bootstrap epistemic uncertainty estimator

$$\begin{aligned} I_b(X_{\text{test}}, \mathcal{D}_n) &= \mathbb{H}(\mathbb{E}_{(\mathcal{D}_n^b, s)|\mathcal{D}_n}[\hat{p}(\mathcal{D}_n^b, s)]) - \mathbb{E}_{\mathcal{D}_n^b|\mathcal{D}_n}[\mathbb{H}(\mathbb{E}_s[\hat{p}(\mathcal{D}_n^b, s)])] \\ &+ \mathbb{E}_{\mathcal{D}_n^b|\mathcal{D}_n}[\mathbb{H}(\mathbb{E}_s[\hat{p}(\mathcal{D}_n^b, s)])] - \mathbb{E}_{(\mathcal{D}_n^b, s)|\mathcal{D}_n}[\mathbb{H}(\hat{p}(\mathcal{D}_n^b, s))] \\ &= \underbrace{\mathbb{H}(\mathbb{E}_{\mathcal{D}_n^b|\mathcal{D}_n}[\mathbb{E}_s[\hat{p}(\mathcal{D}_n^b, s)])] - \mathbb{E}_{\mathcal{D}_n^b|\mathcal{D}_n}[\mathbb{H}(\mathbb{E}_s[\hat{p}(\mathcal{D}_n^b, s)])]}_{=: I_b^{\text{resampling}}} \\ &+ \underbrace{\mathbb{E}_{\mathcal{D}_n^b|\mathcal{D}_n}[\mathbb{H}(\mathbb{E}_s[\hat{p}(\mathcal{D}_n^b, s)])] - \mathbb{E}_s[\mathbb{H}(\hat{p}(\mathcal{D}_n^b, s))]}_{=: I_b^{\text{seeds}}}. \quad (3) \end{aligned}$$

$I_b^{\text{resampling}}$  can be viewed as an estimator of the epistemic uncertainty arising due to the randomness in the data sampling process. Intuitively, this represents how much the model prediction would change if different training data had been sampled from the true distribution. On the other hand,  $I_b^{\text{seeds}}$  captures the amount of the entropy difference explained by the variation in the random seeds. That is, this term represents the amount of variation due to the algorithmic randomness. Thus, our proposed estimator can be decomposed into a ‘data sampling’ component and a ‘training randomness’ component.

Next, notice that the estimate of the mutual information from deep ensembles is

$$I^{\text{deep ensemble}} := \mathbb{H}(\mathbb{E}_s[\hat{p}(\mathcal{D}_n, s)]) - \mathbb{E}_s[\mathbb{H}(\hat{p}(\mathcal{D}_n, s))]. \quad (4)$$

This is parallel to the term  $I_b^{\text{seeds}}$  above, but with the full data instead of a bootstrap subsample. Thus, the bootstrap estimator above can be viewed as approximately the MI from random seeds plus an additional term capturing variability in the dataset. In the experiments, we will see that the latter is often smaller than the former. In this way,

$$I_b(X_{\text{test}}, \mathcal{D}_n) \approx I^{\text{deep ensemble}}.$$

This link gives a new frequentist motivation for deep ensembles. More precisely, since Sec. 3.3 proved that the bootstrap estimator is asymptotically correct for the true Bayesian target, the above relation indicates how deep ensembles succeed in capturing the Bayesian MI.

## 4. Experiments

Section 3.4 gives us a way to measure contributions to epistemic uncertainty from sampling variability in the training data and from stochasticity in the training procedure; as well as a measure for the epistemic uncertainty in a deep ensemble. Our empirical investigations now seek to address two questions—

1. Does training randomness ( $I_b^{\text{seeds}}$  in eq. 3) contribute more to epistemic uncertainty than data sampling ( $I_b^{\text{resampling}}$  in eq. 3)?
2. Does the deep ensemble ( $I^{\text{deep ensemble}}$  in eq. 4) capture the training randomness ( $I_b^{\text{seeds}}$ )?

### 4.1. Experimental Setup

We will use the same experimental setup across various deep learning classification tasks. We first train a deep ensemble of  $B$  models on the entire training dataset. We use this to estimate  $I^{\text{deep ensemble}}$  for each test point by approximating expectations with empirical averages in eq. 4. Next, we construct  $B$  bootstrapped versions of the training dataset and train a deep ensemble of size  $B$  on each. We use these deep ensembles to similarly estimate  $I_b^{\text{seeds}}$  and  $I_b^{\text{resampling}}$  for each test point.

### 4.2. Evaluation Metrics

To answer the first question, we look at the slope of the line of best fit ( $m$  when  $y = mx$ ) that regresses  $I_b^{\text{resampling}}$  on  $I_b^{\text{seeds}}$ ; we shall refer to this slope as  $m_{\text{seeds}}^{\text{resampling}}$ . Fig. 2 visualizes this line in red. This tells us how the magnitude of  $I_b^{\text{resampling}}$  compares to  $I_b^{\text{seeds}}$  on average. For the second question, we again look at the slope of the line of best fit that regresses  $I^{\text{deep ensemble}}$  on  $I_b^{\text{seeds}}$  to compare the relative magnitudes of the two; we shall refer to this slope as  $m_{\text{seeds}}^{\text{deep ensemble}}$ . Fig. 3 (right) visualizes this line in orange. We also look at the Spearman rank correlation between  $I^{\text{deep ensemble}}$  and  $I_b^{\text{seeds}}$  to evaluate if points with high relative epistemic uncertainty due to training stochasticity also exhibit high relative epistemic uncertainty when we use deep ensembles; we shall refer to this correlation as  $\rho$ . This is particularly insightful since performance on many downstream tasks (such as AUC-ROC in outlier detection tasks) often only depends on the ordering of test points rather the explicit magnitudes of the uncertainty estimates.

### 4.3. Deep Learning Tasks

To lend robustness to our empirical findings, we study performance across four tasks spanning various data domains (natural images, medical images, text), different dataset sizes (1000 classes and  $> 1\text{M}$  training examples, 2 classes and 1000 training examples) and different deep learning regimes (training from scratch, fine-tuning, transfer learning). For each task, we defer hyperparameter details and accuracy metrics to Appendix B.1.

#### 4.3.1. CIFAR-10

We train a ResNet-18 (He et al., 2015) from scratch on the CIFAR-10 dataset (Krizhevsky, 2009) which consists of 50,000 training examples spanning 10 classes of natural

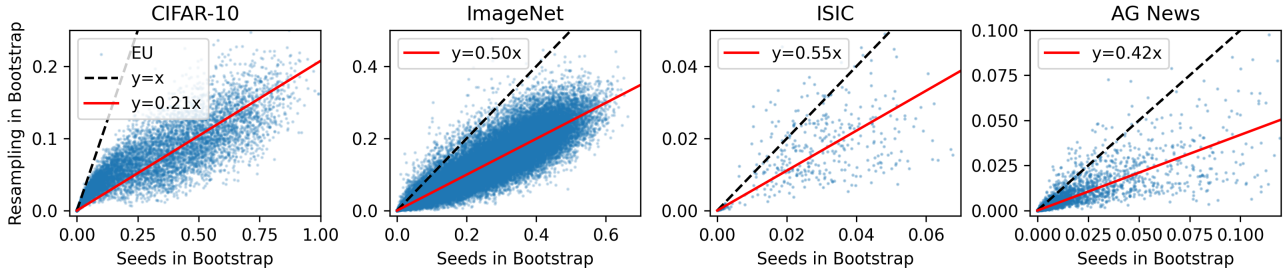


Figure 2. **Uncertainty Components of Bootstrap Estimator:** Scatter plot of epistemic uncertainty due to training stochasticity ( $I_b^{\text{seeds}}$ ) versus epistemic uncertainty due to data resampling ( $I_b^{\text{resampling}}$ ) along with line of best fit in red. See Sec. 4.2 for details.

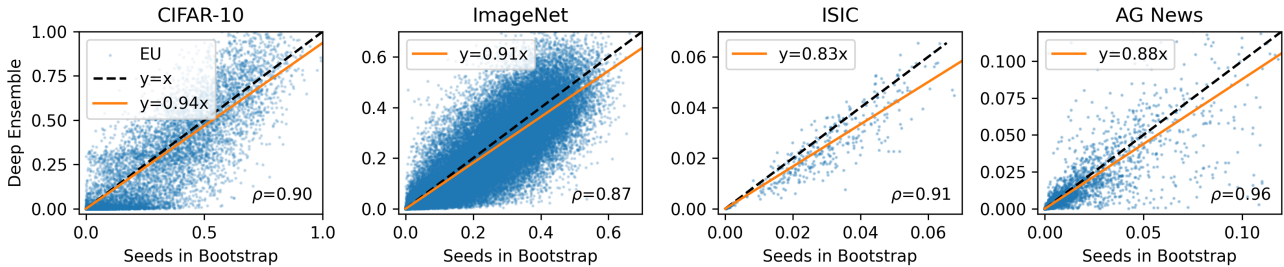


Figure 3. **Uncertainty due to Training Stochasticity:** Scatter plot of epistemic uncertainty due to training stochasticity ( $I_b^{\text{seeds}}$ ) versus deep ensemble estimate of epistemic uncertainty ( $I_b^{\text{deep ensemble}}$ ) along with line of best fit (orange) and spearman correlation ( $\rho$ ). See Sec. 4.2 for details.

images. We use ensembles of size 10.

#### 4.3.2. IMAGENET

We train a ResNet-18 (He et al., 2015) from scratch on the ImageNet dataset (Deng et al., 2009) which consists of 1.28M training examples spanning 1000 classes of natural images. Due to computational limitations, we use ensembles of size 4.

#### 4.3.3. ISIC SKIN LESION DATASET

The ISIC (International Skin Imaging Collaboration) 2016 skin lesion challenge (Gutman et al., 2016) consists of a dataset of images of skin lesions. There are only 900 training images spanning two classes (benign and malignant) in this dataset. For such small datasets, transfer learning (Pan & Yang, 2010) is a common approach wherein a pretrained model from a similar task is used to extract features for the task of interest. More precisely, we use the pretrained ResNet-50 model from He et al. (2015) to extract 2048-dimensional feature vectors. We then train a two layer MLP from random initialization on top of these feature vectors to perform binary classification. We use ensembles of size 10.

#### 4.3.4. AG NEWS DATASET

The AG news topic classification dataset (Zhang et al., 2015) consists of 120,000 news articles (titles and descriptions)

Table 1. Slope of line of best fit from  $I_b^{\text{resampling}}$  on  $I_b^{\text{seeds}}$  ( $m_{\text{seeds}}^{\text{resampling}}$ ), from  $I_b^{\text{deep ensemble}}$  on  $I_b^{\text{seeds}}$  ( $m_{\text{seeds}}^{\text{deep ensemble}}$ ) and spearman correlation between  $I_b^{\text{deep ensemble}}$  and  $I_b^{\text{seeds}}$  ( $\rho$ ). See Sec. 4.2 for details.

DATASET	$m_{\text{SEEDS}}^{\text{RESAMPLING}}$	$m_{\text{SEEDS}}^{\text{DEEP ENSEMBLE}}$	$\rho$
CIFAR-10	0.21	0.94	0.90
IMAGENET	0.50	0.91	0.87
ISIC	0.55	0.83	0.91
AG NEWS	0.42	0.88	0.96

spanning 4 categories. As is common in natural language processing (NLP), we finetune a pretrained model to perform classification. Specifically, we finetune the TinyBERT (Jiao et al., 2020) model which has a transformer architecture (14.5M parameters) for classification by adding a linear layer (initialized randomly) on top of the transformer layers to perform classification. We use ensembles of size 10.

## 4.4. Results

Fig. 2 visualizes scatter plots of  $I_b^{\text{seeds}}$  versus  $I_b^{\text{resampling}}$  along with the line of best fit (slope =  $m_{\text{seeds}}^{\text{resampling}}$ ) with numerical values of the slopes in Table 1.  $I_b^{\text{seeds}}$  always dominates over  $I_b^{\text{resampling}}$ , with the latter being between 0.2 and 0.5 times of the former on average. Therefore, training randomness contributes more to epistemic uncertainty than variability in data sampling. From a model development perspective, this

indicates that if practitioners want to reduce their prediction uncertainty it may be more fruitful to train a bigger deep ensemble to target the uncertainty due to stochastic training, than to collect more data to target the uncertainty due to variability in data sampling.

Fig. 3 visualizes scatter plots of  $I_b^{\text{seeds}}$  versus  $I_b^{\text{deep ensemble}}$  along with the line of best fit (slope =  $m_{\text{seeds}}^{\text{deep ensemble}}$ ) with numerical values of the slopes and correlation in Table 1.  $I_b^{\text{seeds}}$  and  $I_b^{\text{deep ensemble}}$  have similar magnitudes (around 90% of each other) and correlate well ( $\rho \approx 0.9$ ). Therefore, deep ensembles do indeed capture the uncertainty due to training randomness. Together, these observations allow us to conclude that deep ensembles succeed by capturing the majority portion (training randomness) of an asymptotically correct estimator ( $I_b(X_{\text{test}}, \mathcal{D}_n)$ ) of the Bayesian epistemic uncertainty.

## 5. Related Work

### 5.1. Uncertainty Decomposition

MI as a measure of epistemic uncertainty has demonstrated success in active learning (Houlsby et al., 2011; Gal et al., 2017), out-of-distribution and misclassification detection tasks (Kotelevskii et al., 2025). Beyond the specific information theoretic uncertainty decomposition considered in our work, a variety of other ways of quantifying epistemic uncertainty have also been proposed (Senge et al., 2014; Kendall & Gal, 2017; Hofman et al., 2024; Lahlou et al., 2023; Schweighofer et al., 2023; Smith et al., 2025) and MI does have drawbacks (Wimmer et al., 2023). See Hüllermeier & Waegeman (2021) for a comprehensive review of the topic. Indeed, epistemic and aleatoric uncertainty are often not cleanly separable and take on different meanings in different contexts (Kirchhof et al., 2025). We use MI for our investigations because of its widespread use, strong conceptual foundation and practical success; our work is not intended to address the optimality of MI as an epistemic uncertainty assessment.

Similar to our work, Huang et al. (2023) and Neal et al. (2019) also decompose the variance in model predictions for regression tasks into data variability and training randomness components. However, quite different to our contribution, Huang et al. (2023) used this decomposition to study ways of theoretically eliminating training randomness using the NTK approximation (Jacot et al., 2018), while Neal et al. (2019) used this decomposition to investigate the bias-variance tradeoff.

### 5.2. Bayesian and Frequentist Equivalence

Rubin (1981) considers bootstrap from a Bayesian lens, although this interpretation is hard to reconcile with tradi-

tional Bayesian inference since it considers priors over the data rather than the parameters. Closest to our theoretical results is the work by Newton & Raftery (1994) which studied the use of bootstrap as a way of generating samples from a Bayesian posterior. Our work expands upon this idea by specifically leveraging this connection to connect frequentist and Bayesian notions of uncertainty. Moreover, we operationalize this idea in a modern context with DNNs and use it to study deep ensembles. Finally, Fong et al. (2023) also connects Bayesian parameter uncertainty to frequentist uncertainty arising due to lack of data. While their work conceptually shares connections to ours, it consider different practical applications.

### 5.3. Deep Ensembles

The uncertainty quantification capabilities of deep ensembles (Lakshminarayanan et al., 2017) were studied in depth by Ovadia et al. (2019) and Ashukha et al. (2020). Broadly speaking, these studies observed that deep ensembles have well calibrated probabilistic forecasts both in and out-of-domain, and exhibit strong performance on downstream tasks such as out-of-distribution detection and misclassification detection.

Several reasons behind their success have been put forth (Fort et al., 2020), including Bayesian ones (Wilson & Izmailov, 2020). These works primarily note that members of a deep ensemble capture different modes of the loss landscape and can be seen as high quality samples from the posterior. Our work is complementary to this perspective and provides a frequentist understanding of what uncertainties deep ensembles capture.

### 5.4. Bootstrapping for Uncertainties in Deep Learning

The idea of using bootstrap to estimate uncertainties in machine learning has been explored by several works in different contexts. Jürgens et al. (2024) investigates the suitability of evidential deep learning (Sensoy et al., 2018) for uncertainty quantification by comparing them to the bootstrapped estimates of the model parameters, which they believe accurately capture uncertainty in model predictions due to randomness in the training data. Jiménez et al. (2025) investigates variance based measures of uncertainty in a regression setting to also note that deep ensembles only capture uncertainty due to training variability which often dominates over uncertainty due to randomness in training data, similar to our findings in Sec. 4. Lastly, Shaker & Hüllermeier (2020) have also considered approximating the posterior distribution by the trees in a random forest, which can be seen as bootstrap estimates, for the purposes of mutual information estimation as in our work.

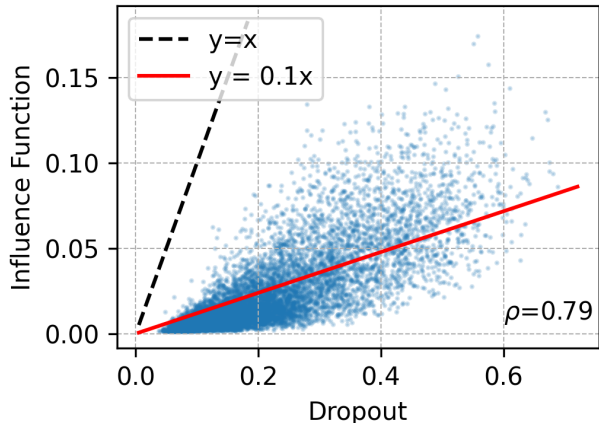


Figure 4. **Influence Function Approximation:** Estimates of epistemic uncertainty using Dropout, versus using influence functions to approximate predictions from bootstrapped datasets.

## 6. Discussion

### 6.1. Limitations

Theorem 3.2 only proves the asymptotic validity of the bootstrap estimator which can weaken the theoretical link between deep ensembles and Bayesian inference in low data regimes. Furthermore, our theorems also rely on assumptions that can be unrealistic in practical settings. In particular, correct specification of the model and identifiability of parameters can certainly appear tenuous for DNNs. Finally, while we aimed to cover a wide range of deep learning settings in our empirical studies, we recognize that more evaluation can always be carried out to lend robustness to our conclusions.

### 6.2. Future Directions

We identify an interesting link between the bootstrap estimator in Sec. 3.3 and data attribution methods such as influence functions (Hampel et al., 2011; Koh & Liang, 2017; Giordano et al., 2019) and datamodels (Ilyas et al., 2022; Park et al., 2023) which aim to identify training data points most responsible for a model’s predictions. These methods allow for estimation of predictions under perturbation of training data and can therefore be used to approximate the predictions of a model trained on bootstrapped data needed for our proposed measure. Any data attribution algorithm that yields a mapping from training data to model predictions can be leveraged to estimate the variance terms in (2), and hence give epistemic uncertainty estimates. We investigate the performance of such an MI estimate based on influence functions; see Appendix B.2 for a similar experiment with datamodels and hyperparameter details.

We train a single convolutional network called the LeNet-5 on MNIST data (LeCun et al., 1998). Next, we calculate

the influence functions for each data point as described in Koh & Liang (2017) for the model parameters in the last two fully connected layers. For each data point, we multiply the influence function by the change in the weighting under bootstrap and add all these products to the parameters to obtain an approximation for model parameters under a bootstrap reweighting. We obtain predictions from 100 such approximated models and use Algorithm 1 to obtain MI estimates. To obtain a Bayesian estimate of MI, we follow the Bayesian interpretation of Monte Carlo Dropout proposed in Gal & Ghahramani (2016) wherein Dropout is enabled at inference time and stochastic forward passes are performed to obtain samples from the Bayesian predictive distribution.

Fig. 4 shows the influence function approximation and Dropout estimates. While there is correlation, influence function estimates are an order of magnitude smaller. We hypothesize that this is because the influence function approximation only uses a single trained model and hence fails to capture the randomness due to training stochasticity.

Nonetheless, our experiment serves as proof-of-concept for studying “uncertainty attribution”—identifying data points or modalities responsible for model uncertainty—by estimating their influence function. Since the variance of an estimator is equal to variance of its influence function (Tsiatis, 2007), we can note that training data points with high influence on a test prediction drive up the variance of the influence function and hence lead to higher epistemic uncertainty. We hope to explore this more in a future work.

## 7. Conclusion

Our paper aims to investigate the uncertainty quantification capabilities of deep ensembles from a frequentist perspective. Specifically, we study the epistemic uncertainty captured by deep ensembles, as measured by the mutual information between the model parameters and the data label. We derive an asymptotic expansion for this mutual information and use it to motivate the construction of an asymptotically correct bootstrap based estimator. Bayesian formulations cannot account for randomness in model parameter selection, while deep ensembles exclusively make use of this randomness. To bridge this gap, we make use of the bootstrap estimator—we show how the bootstrap estimate can be seen as an additive composition of the uncertainty from training randomness and uncertainty due to data sampling. We then conduct empirical studies which establish that training randomness dominates over data sampling, and that deep ensemble estimates of epistemic uncertainty closely capture the training randomness. Therefore, our investigations indicate that deep ensembles succeed at uncertainty quantification tasks by targeting the dominant contribution to an asymptotically correct estimate of the true Bayesian epistemic uncertainty.

## Impact Statement

This paper presents work whose goal is to advance the field of Machine Learning. There are many potential societal consequences of our work, none which we feel must be specifically highlighted here.

## References

- Ashukha, A., Lyzhov, A., Molchanov, D., and Vetrov, D. Pitfalls of in-domain uncertainty estimation and ensembling in deep learning. In *International Conference on Learning Representations*, 2020. URL <https://openreview.net/forum?id=BJxI5gHKDr>.
- Chrabaszcz, P., Loshchilov, I., and Hutter, F. A downsampled variant of imagenet as an alternative to the cifar datasets, 2017. URL <https://arxiv.org/abs/1707.08819>.
- Deng, J., Dong, W., Socher, R., Li, L.-J., Li, K., and Fei-Fei, L. Imagenet: A large-scale hierarchical image database. In *Computer Vision and Pattern Recognition, 2009. CVPR 2009. IEEE Conference on*, pp. 248–255, 2009.
- Depeweg, S., Hernandez-Lobato, J.-M., Doshi-Velez, F., and Udluft, S. Decomposition of uncertainty in bayesian deep learning for efficient and risk-sensitive learning. In *International conference on machine learning*, pp. 1184–1193. PMLR, 2018.
- Efron, B. Bootstrap Methods: Another Look at the Jackknife. *The Annals of Statistics*, 7(1):1 – 26, 1979. doi: 10.1214/aos/1176344552. URL <https://doi.org/10.1214/aos/1176344552>.
- Fong, E., Holmes, C., and Walker, S. G. Martingale posterior distributions. *Journal of the Royal Statistical Society Series B: Statistical Methodology*, 85(5):1357–1391, 2023.
- Fort, S., Hu, H., and Lakshminarayanan, B. Deep ensembles: A loss landscape perspective, 2020. URL <https://arxiv.org/abs/1912.02757>.
- Gal, Y. and Ghahramani, Z. Dropout as a bayesian approximation: Representing model uncertainty in deep learning. In Balcan, M. F. and Weinberger, K. Q. (eds.), *Proceedings of The 33rd International Conference on Machine Learning*, volume 48 of *Proceedings of Machine Learning Research*, pp. 1050–1059, New York, New York, USA, 20–22 Jun 2016. PMLR. URL <https://proceedings.mlr.press/v48/gall16.html>.
- Gal, Y., Islam, R., and Ghahramani, Z. Deep bayesian active learning with image data. In *International conference on machine learning*, pp. 1183–1192. PMLR, 2017.
- Giordano, R., Stephenson, W., Liu, R., Jordan, M., and Broderick, T. A swiss army infinitesimal jackknife. In Chaudhuri, K. and Sugiyama, M. (eds.), *Proceedings of the Twenty-Second International Conference on Artificial Intelligence and Statistics*, volume 89 of *Proceedings of Machine Learning Research*, pp. 1139–1147. PMLR, 16–18 Apr 2019. URL <https://proceedings.mlr.press/v89/giordano19a.html>.
- Graves, A. Practical variational inference for neural networks. *Advances in neural information processing systems*, 24, 2011.
- Gutman, D., Codella, N. C. F., Celebi, E., Helba, B., Marchetti, M., Mishra, N., and Halpern, A. Skin lesion analysis toward melanoma detection: A challenge at the international symposium on biomedical imaging (isbi) 2016, hosted by the international skin imaging collaboration (isic), 2016. URL <https://arxiv.org/abs/1605.01397>.
- Hampel, F., Ronchetti, E., Rousseeuw, P., and Stahel, W. *Robust Statistics: The Approach Based on Influence Functions*. Wiley Series in Probability and Statistics. Wiley, 2011. ISBN 9781118150689. URL <https://books.google.com/books?id=XK3uhrVefXQC>.
- He, K., Zhang, X., Ren, S., and Sun, J. Deep residual learning for image recognition. *2016 IEEE Conference on Computer Vision and Pattern Recognition (CVPR)*, pp. 770–778, 2015. URL <https://api.semanticscholar.org/CorpusID:206594692>.
- Hernandez-Lobato, J. M. and Adams, R. Probabilistic back-propagation for scalable learning of bayesian neural networks. In *International conference on machine learning*, pp. 1861–1869. PMLR, 2015.
- Hofman, P., Sale, Y., and Hüllermeier, E. Quantifying aleatoric and epistemic uncertainty: A credal approach. In *ICML 2024 Workshop on Structured Probabilistic Inference { \& } Generative Modeling*, 2024.
- Houlsby, N., Huszár, F., Ghahramani, Z., and Lengyel, M. Bayesian active learning for classification and preference learning. *arXiv preprint arXiv:1112.5745*, 2011.
- Huang, Z., Lam, H., and Zhang, H. Efficient uncertainty quantification and reduction for over-parameterized neural networks. In Oh, A., Naumann, T., Globerson, A., Saenko, K., Hardt, M., and Levine, S. (eds.), *Advances in Neural Information Processing Systems*, volume 36, pp. 64428–64467. Curran Associates, Inc., 2023.
- Hüllermeier, E. and Waegeman, W. Aleatoric and epistemic uncertainty in machine learning: an introduction to concepts and methods. *Machine Learning*, 110

- (3):457–506, March 2021. ISSN 1573-0565. doi: 10.1007/s10994-021-05946-3. URL <http://dx.doi.org/10.1007/s10994-021-05946-3>.
- Ilyas, A., Park, S. M., Engstrom, L., Leclerc, G., and Madry, A. Datamodels: Understanding predictions with data and data with predictions. In *International Conference on Machine Learning*, pp. 9525–9587. PMLR, 2022.
- Jacot, A., Gabriel, F., and Hongler, C. Neural tangent kernel: Convergence and generalization in neural networks. In Bengio, S., Wallach, H., Larochelle, H., Grauman, K., Cesa-Bianchi, N., and Garnett, R. (eds.), *Advances in Neural Information Processing Systems*, volume 31. Curran Associates, Inc., 2018. URL [https://proceedings.neurips.cc/paper\\_files/paper/2018/file/5a4belfa34e62bb8a6ec6b91d2462f5a-Paper.pdf](https://proceedings.neurips.cc/paper_files/paper/2018/file/5a4belfa34e62bb8a6ec6b91d2462f5a-Paper.pdf).
- Jiao, X., Yin, Y., Shang, L., Jiang, X., Chen, X., Li, L., Wang, F., and Liu, Q. TinyBERT: Distilling BERT for natural language understanding. In Cohn, T., He, Y., and Liu, Y. (eds.), *Findings of the Association for Computational Linguistics: EMNLP 2020*, pp. 4163–4174, Online, November 2020. Association for Computational Linguistics. doi: 10.18653/v1/2020.findings-emnlp.372. URL <https://aclanthology.org/2020.findings-emnlp.372/>.
- Jiménez, S., Jürgens, M., and Waegeman, W. Why machine learning models fail to fully capture epistemic uncertainty, 2025. URL <https://arxiv.org/abs/2505.23506>.
- Jürgens, M., Meinert, N., Bengs, V., Hüllermeier, E., and Waegeman, W. Is epistemic uncertainty faithfully represented by evidential deep learning methods? In *Proceedings of the 41st International Conference on Machine Learning*, ICML’24. JMLR.org, 2024.
- Kendall, A. and Gal, Y. What uncertainties do we need in bayesian deep learning for computer vision? *Advances in neural information processing systems*, 30, 2017.
- Kingma, D. P. and Ba, J. Adam: A method for stochastic optimization. In *ICLR*, 2015.
- Kirchhof, M., Kasneci, G., and Kasneci, E. Re-examining the aleatoric and epistemic uncertainty dichotomy. In *ICLR Blogposts 2025*, 2025. <https://iclr-blogposts.github.io/2025/blog/reexamining-the-aleatoric-and-epistemic-uncertainty-dichotomy/>.
- Koh, P. W. and Liang, P. Understanding black-box predictions via influence functions. In *Proceedings of the 34th International Conference on Machine Learning - Volume 70*, ICML’17, pp. 1885–1894. JMLR.org, 2017.
- Kosorok, M. *Introduction to Empirical Processes and Semiparametric Inference*. Springer Series in Statistics. Springer New York, 2007.
- Kotelevskii, N., Kondratyev, V., Takáč, M., Moulines, E., and Panov, M. From risk to uncertainty: Generating predictive uncertainty measures via bayesian estimation. In *The Thirteenth International Conference on Learning Representations*, 2025. URL <https://openreview.net/forum?id=cWfpt2t37q>.
- Krizhevsky, A. Learning multiple layers of features from tiny images. Technical report, University of Toronto, 2009. Unpublished technical report.
- Lahlou, S., Jain, M., Nekoei, H., Butoi, V. I., Bertin, P., Rector-Brooks, J., Korablyov, M., and Bengio, Y. DEUP: Direct epistemic uncertainty prediction. *Transactions on Machine Learning Research*, 2023. ISSN 2835-8856. URL <https://openreview.net/forum?id=eGLdVRvfvfQ>. Expert Certification.
- Lakshminarayanan, B., Pritzel, A., and Blundell, C. Simple and scalable predictive uncertainty estimation using deep ensembles. In *Proceedings of the 31st International Conference on Neural Information Processing Systems, NIPS’17*, pp. 6405–6416, Red Hook, NY, USA, 2017. Curran Associates Inc. ISBN 9781510860964.
- LeCun, Y., Bottou, L., Bengio, Y., and Haffner, P. Gradient-based learning applied to document recognition. *Proceedings of the IEEE*, 86(11):2278–2324, 1998.
- MacKay, D. J. Information-based objective functions for active data selection. *Neural computation*, 4(4):590–604, 1992.
- MacKay, D. J. Probable networks and plausible predictions—a review of practical bayesian methods for supervised neural networks. *Network: computation in neural systems*, 6(3):469, 1995.
- Neal, B., Mittal, S., Baratin, A., Tantia, V., Scicluna, M., Lacoste-Julien, S., and Mitliagkas, I. A modern take on the bias-variance tradeoff in neural networks, 2019. URL <https://arxiv.org/abs/1810.08591>.
- Newton, M. A. and Raftery, A. E. Approximate bayesian inference with the weighted likelihood bootstrap. *Journal of the Royal Statistical Society. Series B (Methodological)*, 56(1):3–48, 1994. ISSN 00359246. URL <http://www.jstor.org/stable/2346025>.
- Ovadia, Y., Fertig, E., Ren, J., Nado, Z., Sculley, D., Nowozin, S., Dillon, J. V., Lakshminarayanan, B., and Snoek, J. Can you trust your model’s uncertainty? evaluating predictive uncertainty under dataset shift. In *Proceedings of the 33rd International Conference on Neural Information Processing Systems*, 2019.

- Pan, S. J. and Yang, Q. A survey on transfer learning. *IEEE Transactions on Knowledge and Data Engineering*, 22 (10):1345–1359, 2010.
- Park, S. M., Georgiev, K., Ilyas, A., Leclerc, G., and Madry, A. Trak: attributing model behavior at scale. In *Proceedings of the 40th International Conference on Machine Learning*, ICML’23. JMLR.org, 2023.
- Rubin, D. B. The Bayesian Bootstrap. *The Annals of Statistics*, 9(1):130 – 134, 1981. doi: 10.1214/aos/1176345338. URL <https://doi.org/10.1214/aos/1176345338>.
- Schweighofer, K., Aichberger, L., Ielanskyi, M., and Hochreiter, S. Introducing an improved information-theoretic measure of predictive uncertainty. *arXiv preprint arXiv:2311.08309*, 2023.
- Senge, R., Bösner, S., Dembczyński, K., Haasenritter, J., Hirsch, O., Donner-Banzhoff, N., and Hüllermeier, E. Reliable classification: Learning classifiers that distinguish aleatoric and epistemic uncertainty. *Information Sciences*, 255:16–29, 2014.
- Sensoy, M., Kaplan, L., and Kandemir, M. Evidential deep learning to quantify classification uncertainty. In Bengio, S., Wallach, H., Larochelle, H., Grauman, K., Cesa-Bianchi, N., and Garnett, R. (eds.), *Advances in Neural Information Processing Systems*, volume 31. Curran Associates, Inc., 2018. URL [https://proceedings.neurips.cc/paper\\_files/paper/2018/file/a981f2b708044d6fb4a71a1463242520-Paper.pdf](https://proceedings.neurips.cc/paper_files/paper/2018/file/a981f2b708044d6fb4a71a1463242520-Paper.pdf).
- Shaker, M. H. and Hüllermeier, E. Aleatoric and epistemic uncertainty with random forests. In Berthold, M. R., Feelders, A., and Kreml, G. (eds.), *Advances in Intelligent Data Analysis XVIII*, pp. 444–456, Cham, 2020. Springer International Publishing. ISBN 978-3-030-44584-3.
- Smith, F. B., Kirsch, A., Farquhar, S., Gal, Y., Foster, A., and Rainforth, T. Prediction-oriented bayesian active learning. In Ruiz, F. J. R., Dy, J. G., and van de Meent, J. (eds.), *International Conference on Artificial Intelligence and Statistics, 25-27 April 2023, Palau de Congressos, Valencia, Spain*, volume 206 of *Proceedings of Machine Learning Research*, pp. 7331–7348. PMLR, 2023. URL <https://proceedings.mlr.press/v206/smith23a.html>.
- Smith, F. B., Kossen, J., Trollope, E., van der Wilk, M., Foster, A., and Rainforth, T. Rethinking aleatoric and epistemic uncertainty. In *Forty-second International Conference on Machine Learning*, 2025. URL <https://openreview.net/forum?id=CY9MlORQs5>.
- Smith, L. N. and Topin, N. Super-convergence: Very fast training of neural networks using large learning rates. In *Artificial intelligence and machine learning for multi-domain operations applications*, volume 11006, pp. 369–386. SPIE, 2019.
- Tsiatis, A. *Semiparametric Theory and Missing Data*. Springer Series in Statistics. Springer New York, 2007. ISBN 9780387373454.
- van der Vaart, A. W. *Asymptotic Statistics*. Cambridge University Press, 2000.
- Welling, M. and Teh, Y. W. Bayesian learning via stochastic gradient langevin dynamics. In *Proceedings of the 28th international conference on machine learning (ICML-11)*, pp. 681–688, 2011.
- Wilson, A. G. and Izmailov, P. Bayesian deep learning and a probabilistic perspective of generalization. In *Proceedings of the 34th International Conference on Neural Information Processing Systems, NIPS ’20*, Red Hook, NY, USA, 2020. Curran Associates Inc. ISBN 9781713829546.
- Wimmer, L., Sale, Y., Hofman, P., Bischl, B., and Hüllermeier, E. Quantifying aleatoric and epistemic uncertainty in machine learning: Are conditional entropy and mutual information appropriate measures? In *Uncertainty in artificial intelligence*, pp. 2282–2292. PMLR, 2023.
- Wolf, T., Debut, L., Sanh, V., Chaumond, J., Delangue, C., Moi, A., Cistac, P., Rault, T., Louf, R., Funtowicz, M., Davison, J., Shleifer, S., von Platen, P., Ma, C., Jernite, Y., Plu, J., Xu, C., Scao, T. L., Gugger, S., Drame, M., Lhoest, Q., and Rush, A. M. Huggingface’s transformers: State-of-the-art natural language processing, 2020. URL <https://arxiv.org/abs/1910.03771>.
- Zhang, X., Zhao, J., and LeCun, Y. Character-level convolutional networks for text classification. In Cortes, C., Lawrence, N., Lee, D., Sugiyama, M., and Garnett, R. (eds.), *Advances in Neural Information Processing Systems*, volume 28. Curran Associates, Inc., 2015. URL [https://proceedings.neurips.cc/paper\\_files/paper/2015/file/250cf8b51c773f3f8dc8b4be867a9a02-Paper.pdf](https://proceedings.neurips.cc/paper_files/paper/2015/file/250cf8b51c773f3f8dc8b4be867a9a02-Paper.pdf).

## A. Proofs

### A.1. Problem Setup and Notation:

We refresh the problem setup and notation below. Consider a supervised learning  $K$ -class classification problem. Specifically,

1. We assume that the training data  $\mathcal{D}_n = \{(X_i, Y_i), i = 1, \dots, n\}$  consists of feature-label pairs, where the features  $X \in \mathcal{X}$  and the labels  $Y \in \{1, \dots, K\}$ .
2. We wish to evaluate the epistemic uncertainty in the prediction for the label  $Y_{\text{test}}$  for the features  $X_{\text{test}}$ .
3. We denote our predictions by  $\hat{p}(X_{\text{test}}; \theta)$  where  $\theta \in \Theta$  our model parameters. Further, denote by  $\hat{p}_k(X_{\text{test}}; \theta)$  the prediction probability assigned to the  $k^{\text{th}}$  class. The model is specified such that  $0 < \hat{p}_k(X_{\text{test}}; \theta) < 1$  and  $\sum_{k=1}^K \hat{p}_k(X_{\text{test}}; \theta) = 1$ .
4. In the Bayesian case, we have a prior  $p(\theta)$  over the parameters and  $p(\theta|\mathcal{D}_n)$  is our posterior. Recall that the epistemic uncertainty measure in the Bayesian case is then

$$\begin{aligned} \mathbb{I}(Y_{\text{test}}; \theta | X_{\text{test}}, \mathcal{D}_n) &= \mathbb{H}(Y_{\text{test}} | X_{\text{test}}, \mathcal{D}_n) - \mathbb{H}(Y_{\text{test}} | \theta, X_{\text{test}}, \mathcal{D}_n) \\ &= \mathbb{H}(\mathbb{E}_{\theta \sim p(\theta|\mathcal{D}_n)}[\hat{p}(X_{\text{test}}; \theta)]) - \mathbb{E}_{\theta \sim p(\theta|\mathcal{D}_n)}[\mathbb{H}(\hat{p}(X_{\text{test}}; \theta))]. \end{aligned}$$

5. In the bootstrap case, we denote our estimate of  $\theta$  over the bootstrapped dataset as  $\hat{\theta}_b$ . We further denote the distribution of this estimate (induced by the randomness in the choice of bootstrap weights) given the data  $\mathcal{D}_n$  as  $p(\hat{\theta}_b|\mathcal{D}_n)$ . Recall that our proposed epistemic uncertainty measure is then

$$\mathbb{I}_b(X_{\text{test}}, \mathcal{D}_n) = \mathbb{H}(\mathbb{E}_{\hat{\theta}_b \sim p_b(\hat{\theta}_b|\mathcal{D}_n)}[\hat{p}(X_{\text{test}}; \hat{\theta}_b)]) - \mathbb{E}_{\hat{\theta}_b \sim p_b(\hat{\theta}_b|\mathcal{D}_n)}[\mathbb{H}(\hat{p}(X_{\text{test}}; \hat{\theta}_b))].$$

The bootstrap weights may be drawn from either a symmetric Dirichlet with concentration parameter 1 or a symmetric multinomial distribution.

### A.2. Assumptions

1.  $\Theta \subset \mathbb{R}^p$  is open.
2. There exists a  $\theta_0 \in \Theta$  such that  $(X_i, Y_i) \stackrel{iid}{\sim} P_X(x)\hat{p}_y(x; \theta_0) =: P_{\theta_0}$ .
3. Assume

$$\psi_{\theta}(x, y) := \left. \frac{\partial \ln(\hat{p}_y(x; \theta))}{\partial \theta} \right|_{\theta=\theta}$$

exists everywhere. Further assume  $\mathbb{E}_{(x,y) \sim P_{\theta_0}}[\psi_{\theta_0}(x, y)] = 0$ .

4.  $\mathbb{E}_{(x,y) \sim P_{\theta_0}}[|\psi_{\theta_0}(x, y)|^2] < \infty$ . Further,  $\mathbb{E}_{(x,y) \sim P_{\theta_0}}[\psi_{\theta_0}(x, y)]$  is differentiable at  $\theta_0$  with non singular derivative matrix  $-\mathcal{I}(\theta_0)$ . The model is sufficiently smooth such that  $\mathbb{E}_{(x,y) \sim P_{\theta_0}}[\psi_{\theta_0}(x, y)\psi_{\theta_0}(x, y)^T] = \mathcal{I}(\theta_0)$ .
5. The prior  $p(\theta)$  is absolutely continuous with respect to the Lebesgue measure in a neighborhood of  $\theta_0$ , with a continuous positive density at  $\theta_0$ .
6. For every  $\varepsilon > 0$  there exists a sequence of tests  $\phi_n$  such that

$$P_{\theta_0}^n(\phi_n(\mathcal{D}_n)) \rightarrow 0, \quad \sup_{\|\theta - \theta_0\| \geq 0} P_{\theta_0}^n(1 - \phi_n(\mathcal{D}_n)) \rightarrow 0.$$

7. We further make the following assumption which implies uniform integrability to ensure that the first three moments of the posterior distribution converge

$$\sup_n \mathbb{E}_{\theta \sim p(\theta|\mathcal{D}_n)}[(\sqrt{n}(\hat{p}(X_{\text{test}}; \theta) - \hat{p}(X_{\text{test}}; \theta_0)))^{3+\delta}] < \infty \quad \text{for some } \delta > 0.$$

8. For any sequence  $\{\theta_n\} \in \Theta$ ,  $\mathbb{E}_{(x,y) \sim P_{\theta_0}}[\psi_{\theta_n}(x, y)] \rightarrow 0$  implies  $\|\theta_n - \theta_0\| \rightarrow 0$ .
9. The class  $\{\psi_\theta : \theta \in \Theta\}$  is strong Glivenko-Cantelli.
10. For some  $\eta > 0$ , the class  $\mathcal{F} := \{\psi_\theta : \theta \in \Theta, \|\theta - \theta_0\| \leq \eta\}$  is Donsker and  $\mathbb{E}_{(x,y) \sim P_{\theta_0}}[|\psi_\theta(x, y) - \psi_{\theta_0}(x, y)|^2] \rightarrow 0$  as  $\|\theta - \theta_0\| \rightarrow 0$ .
11. Denote our parameter estimate over the complete dataset as  $\hat{\theta}$ . Then,  $\sum_{i=1}^n \psi_{\hat{\theta}}(X_i, Y_i) = o_p(n^{-1/2})$ . Likewise, for our bootstrap estimate,  $\sum_{i=1}^n \xi_i \psi_{\hat{\theta}_b}(X_i, Y_i) = o_p(n^{-1/2})$  where  $\xi_i, i = 1, \dots, n$  are the bootstrap weights.
12. We again make the following assumption which implies uniform integrability to ensure that the first three moments of the bootstrap distributions converge:

$$\sup_n \mathbb{E}_{\hat{\theta}_b \sim p(\hat{\theta}_b | \mathcal{D}_n)} [(\sqrt{n}(\hat{p}(X_{\text{test}}; \hat{\theta}_b) - \hat{p}(X_{\text{test}}; \theta_0)))^{3+\delta}] < \infty \quad \text{for some } \delta > 0.$$

### A.3. Theorem 1

Under the assumptions 1-7, we have the asymptotic expansion

$$I(Y_{\text{test}}; \theta | X_{\text{test}}, \mathcal{D}_n) = \frac{1}{2n} \sum_{k=1}^K \frac{\sigma_k^2}{\hat{p}_k(X_{\text{test}}; \theta_0)} + o_p(n^{-1}) \quad \forall X_{\text{test}},$$

where  $\sigma_k^2$  is

$$\sigma_k^2 = \left[ \frac{\partial \hat{p}(X_{\text{test}}; \theta_0)^T}{\partial \theta} \mathcal{I}^{-1}(\theta_0) \frac{\partial \hat{p}(X_{\text{test}}; \theta_0)}{\partial \theta} \right]_{k,k},$$

for  $\mathcal{I}^{-1}(\theta_0)$  being the inverse Fisher information of the model at  $\theta_0$ .

#### A.3.1. PROOF

Assume that we have some prior  $p(\theta)$  over our parameters and denote our posterior by  $p(\theta | \mathcal{D}_n)$ . Note that our epistemic uncertainty measure is then

$$\begin{aligned} I(Y_{\text{test}}; \theta | X_{\text{test}}, \mathcal{D}_n) &= H(Y_{\text{test}} | X_{\text{test}}, \mathcal{D}_n) - H(Y_{\text{test}} | \theta, X_{\text{test}}, \mathcal{D}_n) \\ &= H(\mathbb{E}_{\theta \sim p(\theta | \mathcal{D}_n)}[\hat{p}(X_{\text{test}}; \theta)]) - \mathbb{E}_{\theta \sim p(\theta | \mathcal{D}_n)}[H(\hat{p}(X_{\text{test}}; \theta))]. \end{aligned}$$

Our proof proceeds in two parts, we first use Taylor's theorem to find an expansion of the epistemic uncertainty and then we find the asymptotic limit.

Note that  $H$  is infinitely differentiable with first three derivatives given by

$$\begin{aligned} \frac{\partial H(\hat{p})}{\partial \hat{p}_i} &= -1 - \log(\hat{p}_i), \\ \frac{\partial^2 H(\hat{p})}{\partial \hat{p}_i \partial \hat{p}_j} &= \mathbb{I}\{i = j\} \left( \frac{-1}{\hat{p}_i} \right), \\ \frac{\partial^3 H(\hat{p})}{\partial \hat{p}_i \partial \hat{p}_j \partial \hat{p}_k} &= \mathbb{I}\{i = j = k\} \left( \frac{1}{\hat{p}_i^2} \right). \end{aligned}$$

Taylor expanding  $H(\hat{p}(X_{\text{test}}; \theta))$  around  $\mathbb{E}_{\theta \sim p(\theta | \mathcal{D}_n)}[\hat{p}(X_{\text{test}}; \theta)]$  yields

$$\begin{aligned} H(\hat{p}(X_{\text{test}}; \theta)) &= H(\mathbb{E}_{\theta \sim p(\theta | \mathcal{D}_n)}[\hat{p}(X_{\text{test}}; \theta)]) \\ &+ \sum_{k=1}^K (\hat{p}_k(X_{\text{test}}; \theta) - \mathbb{E}_{\theta \sim p(\theta | \mathcal{D}_n)}[\hat{p}_k(X_{\text{test}}; \theta)]) (-1 - \log(\mathbb{E}_{\theta \sim p(\theta | \mathcal{D}_n)}[\hat{p}_k(X_{\text{test}}; \theta)])) \\ &+ \frac{1}{2} \sum_{k=1}^K (\hat{p}_k(X_{\text{test}}; \theta) - \mathbb{E}_{\theta \sim p(\theta | \mathcal{D}_n)}[\hat{p}_k(X_{\text{test}}; \theta)])^2 \left( \frac{-1}{\mathbb{E}_{\theta \sim p(\theta | \mathcal{D}_n)}[\hat{p}_k(X_{\text{test}}; \theta)]} \right) \\ &+ \frac{1}{6} \sum_{k=1}^K (\hat{p}_k(X_{\text{test}}; \theta) - \mathbb{E}_{\theta \sim p(\theta | \mathcal{D}_n)}[\hat{p}_k(X_{\text{test}}; \theta)])^3 \left( \frac{1}{\hat{p}_k^2} \right), \end{aligned}$$

where  $\hat{p}'_k$  is some value between  $\hat{p}_k(X_{\text{test}}; \theta)$  and  $\mathbb{E}_{\theta \sim p(\theta | \mathcal{D}_n)}[\hat{p}_k(X_{\text{test}}; \theta)]$  for  $k = 1, \dots, K$ .

Substituting this back into the expression for epistemic uncertainty yields

$$\begin{aligned}
 & I(Y_{\text{test}}; \theta | X_{\text{test}}, \mathcal{D}_n) \\
 &= \mathbb{H}(\mathbb{E}_{\theta \sim p(\theta | \mathcal{D}_n)}[\hat{p}(X_{\text{test}}; \theta)]) \\
 & - \mathbb{E}_{\theta \sim p(\theta | \mathcal{D}_n)}[\mathbb{H}(\mathbb{E}_{\theta \sim p(\theta | \mathcal{D}_n)}[\hat{p}(X_{\text{test}}; \theta)])] \\
 & - \mathbb{E}_{\theta \sim p(\theta | \mathcal{D}_n)} \left[ \sum_{k=1}^K (\hat{p}_k(X_{\text{test}}; \theta) - \mathbb{E}_{\theta \sim p(\theta | \mathcal{D}_n)}[\hat{p}_k(X_{\text{test}}; \theta)]) (-1 - \log(\mathbb{E}_{\theta \sim p(\theta | \mathcal{D}_n)}[\hat{p}_k(X_{\text{test}}; \theta)]) \right] \\
 & - \frac{1}{2} \mathbb{E}_{\theta \sim p(\theta | \mathcal{D}_n)} \left[ \sum_{k=1}^K (\hat{p}_k(X_{\text{test}}; \theta) - \mathbb{E}_{\theta \sim p(\theta | \mathcal{D}_n)}[\hat{p}_k(X_{\text{test}}; \theta)])^2 \left( \frac{-1}{\mathbb{E}_{\theta \sim p(\theta | \mathcal{D}_n)}[\hat{p}_k(X_{\text{test}}; \theta)]} \right) \right] \\
 & - \frac{1}{6} \mathbb{E}_{\theta \sim p(\theta | \mathcal{D}_n)} \left[ \sum_{k=1}^K (\hat{p}_k(X_{\text{test}}; \theta) - \mathbb{E}_{\theta \sim p(\theta | \mathcal{D}_n)}[\hat{p}_k(X_{\text{test}}; \theta)])^3 \left( \frac{1}{\hat{p}'_k} \right) \right].
 \end{aligned}$$

Note that the first and second term cancel, and the third term is equal to zero. Thus,

$$\begin{aligned}
 I(Y_{\text{test}}; \theta | X_{\text{test}}, \mathcal{D}_n) &= \frac{1}{2} \sum_{k=1}^K \left( \frac{\mathbb{E}_{\theta \sim p(\theta | \mathcal{D}_n)} [(\hat{p}_k(X_{\text{test}}; \theta) - \mathbb{E}_{\theta \sim p(\theta | \mathcal{D}_n)}[\hat{p}_k(X_{\text{test}}; \theta)])^2]}{\mathbb{E}_{\theta \sim p(\theta | \mathcal{D}_n)}[\hat{p}_k(X_{\text{test}}; \theta)]} \right) \\
 & - \frac{1}{6} \sum_{k=1}^K \left( \mathbb{E}_{\theta \sim p(\theta | \mathcal{D}_n)} \left[ \frac{(\hat{p}_k(X_{\text{test}}; \theta) - \mathbb{E}_{\theta \sim p(\theta | \mathcal{D}_n)}[\hat{p}_k(X_{\text{test}}; \theta)])^3}{\hat{p}'_k} \right] \right).
 \end{aligned}$$

Note that the first term above is the variance of the probability predictions divided by the mean prediction under the posterior distribution, i.e.

$$\begin{aligned}
 I(Y_{\text{test}}; \theta | X_{\text{test}}, \mathcal{D}_n) &= \frac{1}{2} \sum_{k=1}^K \left( \frac{\text{Var}_{\theta \sim p(\theta | \mathcal{D}_n)} [\hat{p}_k(X_{\text{test}}; \theta)]}{\mathbb{E}_{\theta \sim p(\theta | \mathcal{D}_n)}[\hat{p}_k(X_{\text{test}}; \theta)]} \right) \\
 & - \frac{1}{6} \sum_{k=1}^K \left( \mathbb{E}_{\theta \sim p(\theta | \mathcal{D}_n)} \left[ \frac{(\hat{p}_k(X_{\text{test}}; \theta) - \mathbb{E}_{\theta \sim p(\theta | \mathcal{D}_n)}[\hat{p}_k(X_{\text{test}}; \theta)])^3}{\hat{p}'_k} \right] \right).
 \end{aligned}$$

Next, we shall evaluate the limit.

Under assumptions 1-7, we can apply the Bernstein-von Mises theorem (van der Vaart (2000) Theorem 10.1). Note that Bernstein von-Mises implies convergence in total variation distance which directly implies convergence in distribution. Hence, we have

$$\sqrt{n}(\theta - \theta_0) | \mathcal{D}_n \xrightarrow{d} \mathcal{N}(0, \mathcal{I}^{-1}(\theta_0)) \quad \text{in } P_{\theta_0}^n\text{-probability.}$$

In particular, the above is short-hand for

$$\sup_{h \in BL_1} \left| \mathbb{E}_{\theta \sim p(\theta | \mathcal{D}_n)} [h(\sqrt{n}(\theta - \theta_0))] - \mathbb{E}_{Z \sim \mathcal{N}(0, \mathcal{I}^{-1}(\theta_0))} [h(Z)] \right| \xrightarrow{P_{\theta_0}^n} 0,$$

where  $BL_1$  is the space of functions  $h : \mathbb{R}^p \mapsto \mathbb{R}$  with Lipschitz norm bounded by 1. Recall that if both expectations on the left hand side were unconditional, limit of the left hand side going to 0 is the standard definition of convergence in distribution. See van der Vaart (2000) Sec. 23.2.1 for further discussion.

We shall henceforth continue with the “ $(\cdot) \xrightarrow{d} (\cdot)$  in  $P_{\theta_0}^n$  probability” notation for ease of exposition.

Note that 3 allows us to apply the functional delta method (see van der Vaart (2000) chapter 20) to evaluate the limit of the function  $\theta \mapsto \hat{p}_k(X_{\text{test}}; \theta)$  under the posterior. This yields,

$$\sqrt{n}(\hat{p}_k(X_{\text{test}}; \theta) - \hat{p}_k(X_{\text{test}}; \theta_0)) | \mathcal{D}_n \xrightarrow{d} \mathcal{N}(0, \sigma_k^2) \quad \text{in } P_{\theta_0}^n\text{-probability,} \quad (5)$$

where  $\sigma_k^2 = \left[ \frac{\partial \hat{p}(X_{\text{test}}; \theta_0)}{\partial \theta} \mathcal{I}^{-1}(\theta_0) \frac{\partial \hat{p}(X_{\text{test}}; \theta_0)}{\partial \theta} \right]_{k,k}$ . Finally, 7 implies uniform integrability allowing us to conclude that the limit of the moment is the moment of the limiting distribution:

$$\mathbb{E}_{\theta \sim p(\theta | \mathcal{D}_n)} [\hat{p}_k(X_{\text{test}}; \theta)] \xrightarrow{P_{\theta_0}^n} \hat{p}_k(X_{\text{test}}; \theta_0),$$

$$\text{Var}_{\theta \sim p(\theta | \mathcal{D}_n)} [\sqrt{n} \hat{p}_k(X_{\text{test}}; \theta)] \xrightarrow{P_{\theta_0}^n} \sigma_k^2.$$

Next, note that  $\hat{p}'_k \in [\hat{p}_k(X_{\text{test}}; \theta), \mathbb{E}_{\theta \sim p(\theta | \mathcal{D}_n)} [\hat{p}_k(X_{\text{test}}; \theta)]]$ . By assumption,  $0 < \hat{p}_k(X_{\text{test}}; \theta) < 1$  and hence  $1/\hat{p}'_k = O_p(1)$ . Furthermore, we also have from equation 5 that  $(\hat{p}_k(X_{\text{test}}; \theta) - \hat{p}_k(X_{\text{test}}; \theta_0)) | \mathcal{D}_n = O_p\left(\frac{1}{\sqrt{n}}\right)$ . Therefore,

$$n \frac{(\hat{p}_k(X_{\text{test}}; \theta) - \mathbb{E}_{\theta \sim p(\theta | \mathcal{D}_n)} [\hat{p}_k(X_{\text{test}}; \theta)])^3}{\hat{p}_k^2} = n O_p\left(\frac{1}{n^{3/2}}\right) O_p(1) = O_p\left(\frac{1}{\sqrt{n}}\right).$$

Again, by the uniform integrability assumption

$$\mathbb{E}_{\theta \sim p(\theta | \mathcal{D}_n)} \left[ n \frac{(\hat{p}_k(X_{\text{test}}; \theta) - \mathbb{E}_{\theta \sim p(\theta | \mathcal{D}_n)} [\hat{p}_k(X_{\text{test}}; \theta)])^3}{\hat{p}_k^2} \right] \xrightarrow{P_{\theta_0}^n} 0.$$

Therefore,

$$nI(Y_{\text{test}}; \theta | X_{\text{test}}, \mathcal{D}_n) \xrightarrow{P_{\theta_0}^n} \frac{1}{2} \sum_{k=1}^K \frac{\sigma_k^2}{\hat{p}_k(X_{\text{test}}; \theta_0)}.$$

#### A.4. Theorem 2

Under the assumptions 1-12,

$$\frac{I(Y_{\text{test}}; \theta | X_{\text{test}}, \mathcal{D}_n)}{I_b(X_{\text{test}}, \mathcal{D}_n)} \xrightarrow{P_{\theta_0}^n} 1 \quad \forall X_{\text{test}},$$

In particular, note that  $I_b$  may be calculated using either symmetric Dirichlet weights with concentration parameter 1, or multinomial weights.

##### A.4.1. PROOF

Recall that our proposed epistemic uncertainty measure for the bootstrap case is

$$I_b(X_{\text{test}}, \mathcal{D}_n) = \mathbb{H}(\mathbb{E}_{\hat{\theta}_b \sim p_b(\hat{\theta}_b | \mathcal{D}_n)} [\hat{p}(X_{\text{test}}; \hat{\theta}_b)]) - \mathbb{E}_{\hat{\theta}_b \sim p_b(\hat{\theta}_b | \mathcal{D}_n)} [\mathbb{H}(\hat{p}(X_{\text{test}}; \hat{\theta}_b))].$$

We can proceed exactly as in the Bayesian case to obtain

$$\begin{aligned} I_b(X_{\text{test}}, \mathcal{D}_n) &= \frac{1}{2} \sum_{k=1}^K \left( \frac{\text{Var}_{\hat{\theta}_b \sim p_b(\hat{\theta}_b | \mathcal{D}_n)} [\hat{p}_k(X_{\text{test}}; \hat{\theta}_b)]}{\mathbb{E}_{\hat{\theta}_b \sim p_b(\hat{\theta}_b | \mathcal{D}_n)} [\hat{p}_k(X_{\text{test}}; \hat{\theta}_b)]} \right) \\ &\quad - \frac{1}{6} \sum_{k=1}^K \left( \mathbb{E}_{\hat{\theta}_b \sim p_b(\hat{\theta}_b | \mathcal{D}_n)} \left[ \frac{(\hat{p}_k(X_{\text{test}}; \hat{\theta}_b) - \mathbb{E}_{\hat{\theta}_b \sim p_b(\hat{\theta}_b | \mathcal{D}_n)} [\hat{p}_k(X_{\text{test}}; \hat{\theta}_b)])^3}{\hat{p}_k^2} \right] \right), \end{aligned}$$

where  $\hat{p}'_k$  is now some value between  $\hat{p}_k(X_{\text{test}}; \hat{\theta}_b)$  and  $\mathbb{E}_{\hat{\theta}_b \sim p_b(\hat{\theta}_b | \mathcal{D}_n)} [\hat{p}_k(X_{\text{test}}; \hat{\theta}_b)]$  for  $k = 1, \dots, K$ . Next, from Theorem 10.16 of Kosorok (2007), we have

$$\sqrt{n} (\hat{\theta}_b - \hat{\theta} | \mathcal{D}_n) \xrightarrow{d} \mathcal{N}(0, \mathcal{I}^{-1}(\theta_0)) \quad \text{in } P_{\theta_0}^n\text{-probability}$$

and

$$\sqrt{n} (\hat{\theta} - \theta_0) \xrightarrow{d} \mathcal{N}(0, \mathcal{I}^{-1}(\theta_0)),$$

where  $\hat{\theta}$  is the MLE over the complete data. Notably, both the statements above hold for either multinomial or Dirichlet weights.

We can now apply the delta method for bootstrap (van der Vaart (2000) Theorem 23.9) to this and proceed exactly as in the Bayesian case to conclude

$$n\mathbb{I}_b(X_{\text{test}}, \mathcal{D}_n) \xrightarrow{P_{\theta_0}^n} \frac{1}{2} \sum_{k=1}^K \frac{\sigma_k^2}{\hat{p}_k(X_{\text{test}}; \theta_0)}.$$

Combining the Bayesian and bootstrap results by the continuous mapping theorem,

$$\frac{n\mathbb{I}(Y_{\text{test}}; \theta | X_{\text{test}}, \mathcal{D}_n)}{n\mathbb{I}_b(X_{\text{test}}, \mathcal{D}_n)} \xrightarrow{P_{\theta_0}^n} 1.$$

## B. Additional Experiments and Experimental Details

### B.1. Epistemic Uncertainty Decomposition

#### B.1.1. CIFAR-10

**Experimental Details:** We use the CIFAR-10 dataset (Krizhevsky, 2009) with the original training and test set folds. We use a standard ResNet-18 (He et al., 2015) architecture but modify the first convolutional layer to have a kernel size of 3, stride of 1, padding of 1 to allow the network to work with  $32 \times 32$  size images. Further, we modify the last fully connected layer to only have 10 output neurons for a 10 class classification task. We use cross entropy loss and Adam (Kingma & Ba, 2015) as an optimizer with learning rate of 0.001 and betas of 0.9 and 0.999. We use a batch size of 128 and train for 15 epochs. The rest of the experiment proceeds as described in the main text.

**Accuracy Metrics:** Models within the deep ensemble achieve an accuracy of 0.83 on average, whereas the bootstrap models achieve an accuracy of 0.80 on average. The deep ensemble itself (i.e. averaged model predictions) achieves an accuracy of 0.89. Deep ensembles over the bootstrapped datasets (i.e. model predictions averaged over the random seeds only) achieves an accuracy of 0.88 on average across the bootstrapped datasets.

#### B.1.2. IMAGENET

**Experimental Details:** We use the ImageNet dataset (Deng et al., 2009) with the original training and test set folds. For computational ease, we use a downsampled version of the images downsampled to  $32 \times 32$  pixels as in Chrabaszcz et al. (2017). We use a standard ResNet-18 (He et al., 2015) architecture but modify the first convolutional layer to have a kernel size of 3, stride of 1, padding of 1 to allow the network to work with  $32 \times 32$  size images. We use cross entropy loss and SGD as an optimizer with learning rate of 0.1, momentum of 0.9 and weight decay of 0.0001. We use a batch size of 128 and train for 40 epochs. We use the one cycle learning rate policy from Smith & Topin (2019). The rest of the experiment proceeds as described in the main text.

**Accuracy Metrics:** Models within the deep ensemble achieve top-1 and top-5 accuracy of 0.55 and 0.79 respectively on average, whereas the bootstrap models achieve top-1 and top-5 accuracies of 0.51 and 0.75 respectively on average. The deep ensemble itself (i.e. averaged model predictions) achieves top-1 and top-5 accuracy of 0.59 and 0.81 respectively. Deep ensembles over the bootstrapped datasets (i.e. model predictions averaged over the random seeds only) achieves top-1 and top-5 accuracy of 0.55 and 0.78 on average across the bootstrapped datasets.

#### B.1.3. ISIC DATASET

**Experimental Details:** We use the ISIC Skin Lesion challenge (2016) dataset (Gutman et al., 2016) with the original training and test set folds. We pass all images through the trained ResNet-50 from He et al. (2015) and extract the activations from the last layer to obtain 2048-dimensional feature vectors. We then train a two layer neural network from scratch on top of these feature vectors with 512 hidden units, ReLU activation and Dropout with a rate of 0.5. We use Adam (Kingma & Ba, 2015) as an optimizer with a learning rate of 0.001 and betas of 0.9 and 0.999. We use a batch size of 32 and train for 15 epochs minimizing cross entropy loss weighted by prevalence of ground truth class prevalence in training data to account for class imbalance. The rest of the experiment proceeds as described in the main text.

**Accuracy Metrics:** Models within the deep ensemble achieve an AUC-ROC of 0.81 on average, whereas the bootstrap models achieve an accuracy of 0.79 on average. The deep ensemble itself (i.e. averaged model predictions) achieves an accuracy of 0.81. Deep ensembles over the bootstrapped datasets (i.e. model predictions averaged over the random seeds only) achieves an accuracy of 0.80 on average across the bootstrapped datasets.

#### B.1.4. AG NEWS

**Experimental Details:** We use the AG News dataset (Zhang et al., 2015) with the original training and test set folds. We finetune the TinyBERT model from Jiao et al. (2020). We add a linear layer on top of the final 312 dimensional output from TinyBERT to perform 4 class classification (parameters initialized randomly). We use Adam (Kingma & Ba, 2015) as an optimizer with a learning rate of  $2e - 5$  and betas of 0.9 and 0.999. We also use a linear learning rate schedule with warmup as provided by the transformers (Wolf et al., 2020) library. We train for 3 epochs with a batch size of 32. We tokenize each example up to 128 tokens, padding or truncating as necessary. The rest of the experiment proceeds as described in the main text.

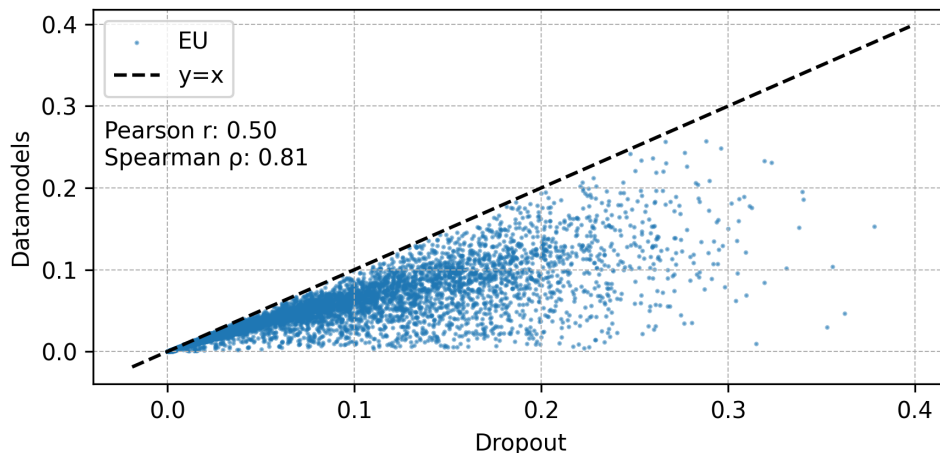


Figure 5. **Datamodels Approximation:** Datamodel approximation to our measure versus mutual information estimates obtained using Dropout on CIFAR-10 test points. See text for details.

**Accuracy Metrics:** Models within the deep ensemble achieve an accuracy of 0.94 on average, whereas the bootstrap models achieve an accuracy of 0.93 on average. The deep ensemble itself (i.e. averaged model predictions) achieves an accuracy of 0.94. Deep ensembles over the bootstrapped datasets (i.e. model predictions averaged over the random seeds only) achieves an accuracy of 0.93 on average across the bootstrapped datasets.

## B.2. Data Attribution

**Experimental Details:** We use the MNIST dataset (LeCun et al., 1998). For training, we randomly select 600 images from each class to form the training dataset and keep the test dataset the same as the original.

We use a two layer convolutional neural network with 3 fully connected layers. We use Adam (Kingma & Ba, 2015) as an optimizer with a learning rate of 0.001, betas of 0.9 and 0.999, weight decay of 0.0001, and a batch size of 32. We train for 10 epochs.

To calculate the influence function, we freeze all but the final two fully connected layers and calculate the hessian and gradients only with respect to the parameters in these layers. Specifically, as in Koh & Liang (2017), the change in model parameters (for the final two layers) for an  $\epsilon$  increase in the weighting of the  $i^{th}$  training data point is  $-H_{\hat{\theta}}^{-1} \nabla_{\theta} \log(\hat{p}_{Y_i}(X_i; \hat{\theta}))$  where  $\hat{\theta}$  is the MLE on the original (unweighted) dataset,  $H_{\hat{\theta}} = \frac{1}{n} \sum_{i=1}^n \nabla_{\theta}^2 \log(\hat{p}_{Y_i}(X_i; \hat{\theta}))$  is the hessian and  $\nabla_{\theta}$  denotes derivative with respect to  $\theta$ . We use multinomial bootstrap weights. For practical calculation, we add the identity matrix scaled by  $10^{-5}$  to the Hessian to ensure invertibility in cases with non-negative definite hessian—see Koh & Liang (2017) for discussion.

For the Dropout estimate, we add Dropout layers with probability 0.5 between the fully connected layers and train with the same hyperparameters above.

The rest of the experiment proceeds as in the main text.

### B.2.1. DATAMODELS EXPERIMENT

We now also investigate the use of datamodels (Ilyas et al., 2022) as a means of approximating our measure.

**Experimental Details:** We use the CIFAR-10 dataset (Krizhevsky, 2009) and ResNet-9 architecture as in Ilyas et al. (2022). Each test point is associated with a datamodel which consists of a weight vector of length 50001—the number of training data points and a bias term. The datamodel is such that it predicts the model output for that test data point given the weights assigned to the training data as the dot product between the training data weights and the datamodel weights. The model output considered in Ilyas et al. (2022) is unfortunately not the entire probability vector, but simply the difference between the correct logit and the highest incorrect logit. For our experiment, we use the datamodels for CIFAR-10 provided as part of the paper—see Ilyas et al. (2022) for details. We then draw 100 sets of Dirichlet weights and obtain estimates of model

outputs using the datamodel. We then pass the model output through the sigmoid function to obtain a probability and use this for calculation of the EU. Note that this is equivalent to treating the classification task as binary between the correct class vs the highest incorrect class. While this is not equivalent to the correct calculation of EU over the 10 class probability vector, it is the best we can do with the existing datamodel.

For the dropout estimate, we train a ResNet-9 with Dropout layers added with probability 0.5 with the exact same hyperparameters used to create the datamodel.

**Results:** Fig. 5 shows that the datamodels approximation to our measure and the Dropout epistemic uncertainty scores have a high rank correlation and moderate Pearson correlation. The datamodel estimates are also consistently lower than the Dropout estimates. This may be because of the reduction to a binary classification task in the Datamodels approximation versus the full 10 class classification in the Dropout calculation. Nonetheless, this is a useful proof of concept experiment which opens the door to using data attribution methods for a more nuanced understanding of sources of uncertainty .